Acta Crystallographica Section D
**Biological Crystallography**
ISSN 0907-4449

# Structural characterization and comparison of RGD cell-adhesion recognition sites engineered into streptavidin

**Isolde Le Trong,[a] Todd C. McDevitt,[b] Kjell E. Nelson,[b] Patrick S. Stayton[b] and Ronald E. Stenkamp[a]***

[a]Department of Biological Structure, Biomolecular Structure Center, University of Washington, Seattle, WA 98195, USA, and [b]Department of Bioengineering, University of Washington, Seattle, WA 98195, USA

Correspondence e-mail: stenkamp@u.washington.edu

Received 16 September 2002
Accepted 20 February 2003

**PDB References:** streptavidin variant containing fibronectin residues (FN-SA), 1mm9, r1mm9sf; streptavidin variant containing osteopontin residues (OPN-SA), 1moy, r1moysf.

The RGD (arginine–glycine–aspartic acid) sequence is found in several important extracellular matrix proteins and serves as an adhesion ligand for members of the integrin family of cell-surface receptors. This sequence and flanking residues from fibronectin or osteopontin have been engineered into an accessible surface loop of streptavidin to create two new streptavidin variants (FN-SA or OPN-SA, respectively) that bind cells through the $\alpha_v\beta_3$ and/or $\alpha_5\beta_1$ integrin receptors. Their crystal structures confirm the design and construction of the mutants and provide evidence about the conformational dynamics of the RGD loops. The loops in the isomorphous crystal structures are involved in crystal-packing interactions and this stabilizes their structures. Even so, the loop in OPN-SA is slightly disordered and two of the residues are not seen in difference electron-density maps. Comparison with other experimentally determined structures of RGD loops in cell-adhesion molecules shows that these loops occupy a large subset of conformational space. This is consistent with the view that RGD loops, at least those involved in cell adhesion, sample a number of structures dynamically, a few of which display high affinity for appropriate receptors.

## 1. Introduction

The ability of cells to adhere to defined extracellular matrix components is tied to many of their biological functions. The extracellular matrix and cell-adhesion proteins include fibronectin, osteopontin, fibrinogen, vitronectin, von Willebrand factor and laminin. These molecules all use integrins as their receptor proteins (Ruoslahti, 1991) and contain a tripeptide motif, Arg-Gly-Asp (RGD), as a ligand sequence that is central to the recognition by the integrin receptors. The residues flanking the RGD motif influence the recognition of the RGD sequence by specific integrins (Pytela *et al.*, 1985; Ruoslahti & Pierschbacher, 1987). In fibronectin, the RGD tripeptide is located in a loop (Leahy *et al.*, 1992, 1996; Dickinson *et al.*, 1994; Leahy, 1997), leading to the general idea that contacts between amino-acid residues in surface loops contribute to many of the protein–protein contacts in cell-adhesion interactions (Smith *et al.*, 1995).

The RGD sequence has been previously introduced into the common adaptor protein streptavidin to expand its technological utility (McDevitt *et al.*, 1999). The tight binding to biotin has made the streptavidin/biotin pair important in a number of biotechnical applications as a linker molecule for joining proteins, DNA, lipids and other molecules. To transfer the cell-adhesion properties of fibronectin and osteopontin to streptavidin, hexapeptides containing the RGD sequence were engineered into the loop region between residues 64 and

| Residue Nos. in wild-type SA | 64 | | 65 | 66 | 67 | | | 68 |
|---|---|---|---|---|---|---|---|---|
| Wild-type SA | Pro | — | Ala | Thr | Asp | — | — | Gly |
| FN-SA | Pro | Gly | Arg | Gly | Asp | Ser | Pro | Gly |
| OPN-SA | Pro | Gly | Arg | Gly | Asp | Ser | Val | Gly |
| Residue Nos. in FN-SA and OPN-SA | 64 | 64A | 65 | 66 | 67 | 67A | 67B | 68 |

**Figure 1**
Sequence alignments for the engineered FN-SA and OPN-SA mutants and wild-type streptavidin. Residues were inserted into the wild-type sequence to generate RGD sequences in this loop (RGD loop). The flanking residues (64A, 67A and 67B) in FN-SA and OPN-SA are those found in wild-type fibronectin and osteopontin, respectively.

68 in the streptavidin sequence (Fig. 1). Other proteins have also been altered to incorporate an RGD site (Maeda *et al.*, 1989; Hashino *et al.*, 1992; Barbas *et al.*, 1993; Rossi *et al.*, 1995; Smith *et al.*, 1995). Insertion of the fibronectin and osteopontin hexapeptides opposite the biotin-binding flexible loop produced bifunctional proteins that possess wild-type biotin dissociation rates and cell-adhesion properties (McDevitt *et al.*, 1999).

We have carried out crystallographic studies of the fibronectin-streptavidin (FN-SA) and osteopontin-streptavidin (OPN-SA) engineered proteins to determine how the protein structure accommodates the inserted residues and to characterize, if possible, the conformations of the RGD motif in these molecules. We have also compared the RGD loops in these molecules with those found in fibronectin and other proteins containing integrin-binding RGD motifs.

## 2. Experimental

### 2.1. Generation of mutants

Construction and production of the mutants FN-SA and OPN-SA has previously been described (McDevitt *et al.*, 1999). Hexapeptide sequences containing the RGD cell-adhesion sequences in fibronectin and osteopontin were engineered into a streptavidin loop near residue 64.

### 2.2. Crystallization

The two mutants were crystallized from solutions containing 20 mg ml$^{-1}$ protein using sitting-drop vapor-diffusion methods. In both cases, crystals grew in 40–50% MPD at room temperature. They grew as tetragonal bipyramids to dimensions of $0.1 \times 0.02 \times 0.02$ mm. The space group for both is $I4_122$, with unit-cell parameters $a = 56.9$, $c = 170.7$ Å. $V_M$ (Matthews, 1968) is 2.51 Å$^3$ Da$^{-1}$, assuming one streptavidin monomer per asymmetric unit. This corresponds to a solvent content of 51%. Streptavidin tetramers can be positioned at sites with 222 crystallographic symmetry with one monomer in the asymmetric unit. The crystals were mounted with 50% MPD in a loop and flash-frozen at 100 K in a nitrogen stream.

**Table 1**
Diffraction data statistics.

Values in parentheses are for the last resolution shell.

| Data set | FN-SA | OPS-SA |
|---|---|---|
| Maximum resolution (Å) | 1.65 (1.68–1.65) | 1.55 (1.58–1.55) |
| Observed reflections | 240518 | 486781 |
| Unique reflections | 17197 | 20871 |
| Completeness (%) | 98.9 (81.4) | 99.9 (99.4) |
| $R_{merge}$ (%) | 0.068 (0.495) | 0.076 (0.593) |
| $\langle I\rangle/\langle\sigma(I)\rangle$ | 28.4 (3.2) | 36.7 (4.2) |

### 2.3. Data collection and processing

Diffraction data were collected at SSRL beamline 9-1 with a MAR Research image-plate scanner. The wavelength was 0.98 Å and the FN-SA and OPS-SA data sets were collected to 1.65 and 1.55 Å resolution, respectively. Data were processed with *DENZO* and merged and scaled with *SCALEPACK* (Otwinowski & Minor, 1997). Data-set statistics are shown in Table 1.

### 2.4. Structure solution and refinement

A model of the N23A mutant of streptavidin without the binding loop (residues 45–51) and solvent molecules was used as the starting point for the FN-SA refinement. Structure refinement was carried out using the program *SHELXL*97 (Sheldrick & Schneider, 1997), its auxiliary program *SHELXPRO* and the graphics program *XTALVIEW* (McRee, 1999).

The structure was refined against $F^2$. All parameters were refined simultaneously and 10% of the data were used for the calculation of $R_{free}$ (Brünger, 1992). Distance, planarity and chiral volume restraints were applied, as were antibumping restraints. The target values for 1–2 and 1–3 distances were based on the Engh & Huber (1991) study.

A full-matrix least-squares rigid-body refinement was first used on the monomer. Subsequently, the model was refined using conjugate-gradient least squares. Similarity restraints were applied for isotropic and anisotropic displacement parameters throughout the refinement.

After adding 35 water molecules based on difference electron-density maps ($|F_o| - |F_c|$), positive density appeared for an MPD molecule in the biotin-binding picket. Density later appeared for the binding loop and another MPD molecule. Negative density for the model in the region of the FN-SA loop appeared for the wild-type model and positive density appeared for the new larger FN-SA loop.

In the final model, the biotin-binding loop residues are in an open conformation, with two MPD molecules in the biotin-binding site. The model contains residues 16–139 plus the three additional residues in the FN-SA loop. 89 solvent molecules are also part of the final model. Alternate conformations for residues 28, 42 and 88 are also included. The reflections used to calculate $R_{free}$ were included in the final refinement step. All of the reflections were used in refinement. The resulting $R$ value is 0.130 for reflections with $|F_o| > 4\sigma(|F_o|)$

**Table 2**
Refinement statistics.

| Structure | FN-SA | OPS-SA |
|---|---|---|
| Maximum resolution (Å) | 20–1.65 | 10–1.55 |
| No. of unique reflections | 17174 | 20741 |
| No. of parameters | 9480 | 9537 |
| No. of restraints | 12020 | 12733 |
| $R_{work}$ | | |
| All reflections | 0.134 | 0.130 |
| $\|F_o\| > 4\sigma(\|F_o\|)$ | 0.119 | 0.122 |
| $R_{free}$ | | |
| All reflections | 0.195 | 0.189 |
| $\|F_o\| > 4\sigma(\|F_o\|)$ | 0.176 | 0.175 |
| $R_{final}$ | | |
| All reflections | 0.145 | 0.132 |
| $\|F_o\| > 4\sigma(\|F_o\|)$ | 0.130 | 0.123 |
| No. of protein atoms | 949 | 970 |
| No. of solvent atoms | 89 | 76 |
| No. of heteroatoms | 16 | 16 |
| Mean $B$ value (isotropic) (Å$^2$) | 23.7 | 24.3 |
| Main-chain atoms | 18.4 | 19.5 |
| Side-chain atoms | 23.3 | 24.4 |
| Solvent and heteroatoms | 42.6 | 42.4 |
| R.m.s. deviations from ideal values | | |
| Bond lengths (Å) | 0.009 | 0.010 |
| Bond angles (Å) | 0.030 | 0.033 |

and 0.145 for all reflections. Refinement statistics are presented in Table 2.

Refinement of OPS-SA followed a similar protocol. The final model includes residues 16–67 and 68–139 with two residues (Ser 67A, Val 67B) missing. The model also contains two MPD molecules in the biotin-binding pocket and 76 water molecules (75 full occupancy, one half-occupied). Two alternate conformations were found for residues 28, 40, 42, 88, 107, 110 and 122. The final $R$ values are 0.123 for reflections with $|F_o| > 4\sigma(|F_o|)$ and 0.132 for all reflections. Refinement statistics are also presented in Table 2.

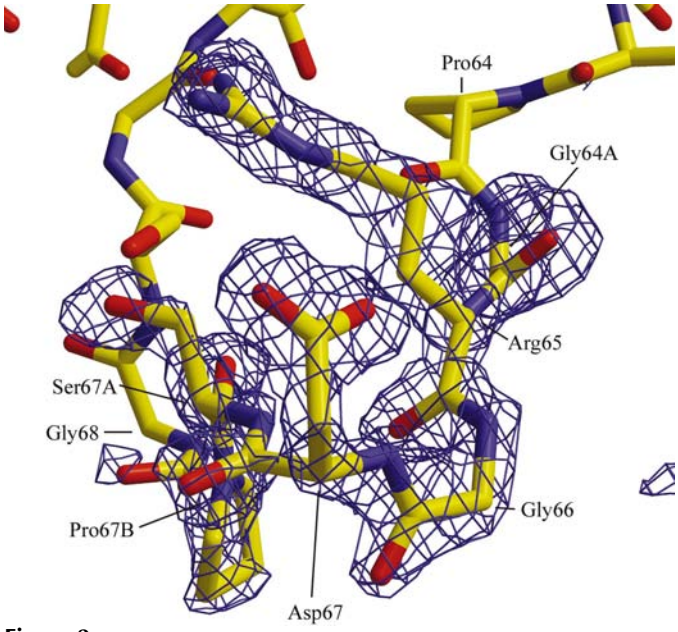


**Figure 2**
Difference electron density ($|F_o| - |F_c|$) used for fitting the loop of residues containing the RGD sequence in FN-SA. The fit model is superposed on the map. The C$^\alpha$ atoms are labeled with residue names and numbers for FN-SA (see Fig. 1). The difference electron density is contoured at 2$\sigma$. Figure drawn using *RASTER3D* (Merritt & Bacon, 1997).

## 3. Results and discussion

Crystallographic refinement of the two proteins at high resolution (1.65 Å for FN-SA and 1.55 Å for OPN-SA) was straightforward and gave final $R$ values of 0.145 for FN-SA and 0.132 for OPN-SA. Ramachandran plots (data not shown) show that no residues have taken on unreasonable main-chain conformations.

Fig. 1 shows the amino-acid sequences in the engineered loops of FN-SA and OPS-SA as well as the residue-numbering scheme used in this paper. Six residues in each mutant were introduced into a loop that contains three residues in wild-type streptavidin. In both mutants, a glycine was included on the N-terminal side of the RGD tripeptide and two residues were added on the C-terminal side. Special residue numbers were assigned to these linking residues to aid in comparisons with other streptavidin molecules.

In the high-resolution model of FN-SA the hexapeptide including the RGD sequence is well defined in difference electron-density maps (Fig. 2), whereas the OPN-SA maps show no clear density for two of the introduced residues (Ser67A and Val67B). These missing residues occur where the FN-SA and OPN-SA sequences differ. In OPN-SA, residue 67B is a valine, while in FN-SA it is a proline. The remaining hexapeptides have the same sequence. Because the model of FN-SA is more complete, much of the following structure analysis and discussion will be based on it.

The overall polypeptide fold of the FN-SA and OPN-SA proteins is very similar to that of wild-type streptavidin (Hendrickson *et al.*, 1989; Weber *et al.*, 1989), with the familiar $\beta$-barrel structure in each monomer and the 222 symmetry of the tetramer. The loop in each streptavidin monomer containing the introduced RGD sequence ('RGD loop') is located on the end of the molecule opposite the biotin-binding site (see Fig. 3). As seen in Fig. 4, the arrangement of the subunits in the tetramer places the RGD loop of one subunit near the biotin-binding site of an adjacent subunit. While close to the binding site, the RGD loop does not significantly alter the biotin-binding characteristics of the protein (McDevitt *et al.*, 1999).

When the FN-SA mutant structure is superposed on that of wild-type streptavidin (Fig. 3), the major structural differences are found in the C-terminal region, the flexible binding loop near residue 48 and the engineered RGD loop.

The C-terminus of the FN-SA is more extended than that of wild-type streptavidin. Owing to crystal-packing interactions, additional residues at the terminus are ordered and observed in the electron-density maps. These residues are within hydrogen-bonding distance of neighboring molecules in the crystals and this stabilizes their more extended conformation.

One component of the protein structure that participates in the tight binding of biotin is the flexible binding loop (residues 45–51; Freitag *et al.*, 1997). This portion of the molecule shows

considerable conformational variation in a number of crystal structures of wild-type and mutant streptavidins. The structure of the loop is influenced by crystal-packing interactions in different crystal forms as well as the presence or absence of liganding molecules in the biotin-binding site. In the case of these two mutants (FN-SA and OPN-SA), the loop is in an open conformation, as found in other unliganded streptavidins.

The third region where the FN-SA structure differs from wild-type streptavidin is in the RGD loop. As shown in Fig. 3, structural differences between polypeptide backbones of the mutants and wild-type streptavidin are minimal at the residues immediately before and after those shown in Fig. 1 (residues 63 and 69 in the wild-type sequence). Any structural adjustments in the wild-type structure, beyond extension of the RGD loop, are local. A more detailed view of the RGD loops in Fig. 5 for FN-SA, OPN-SA and wild-type streptavidin further shows how the additional residues in the loop are accommodated with very little change outside the loop region.

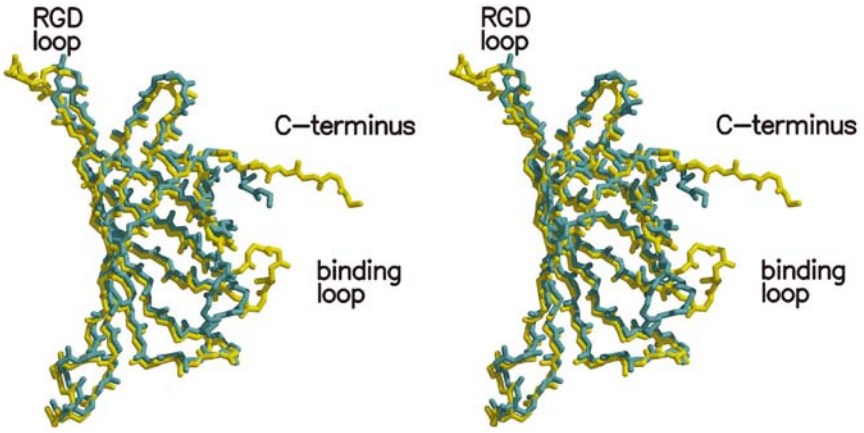


**Figure 3**
Stereoview showing the superposition of the structures of FN-SA and wild-type streptavidin subunits. 65 $C^{\alpha}$ atoms in the $\beta$-barrel core of the monomers were superimposed. Polypeptide backbone atoms for the FN-SA mutant are shown in yellow, while wild-type streptavidin is shown in blue. Figure drawn using *MOLSCRIPT* (Kraulis, 1991) and *RASTER3D* (Merritt & Bacon, 1997).

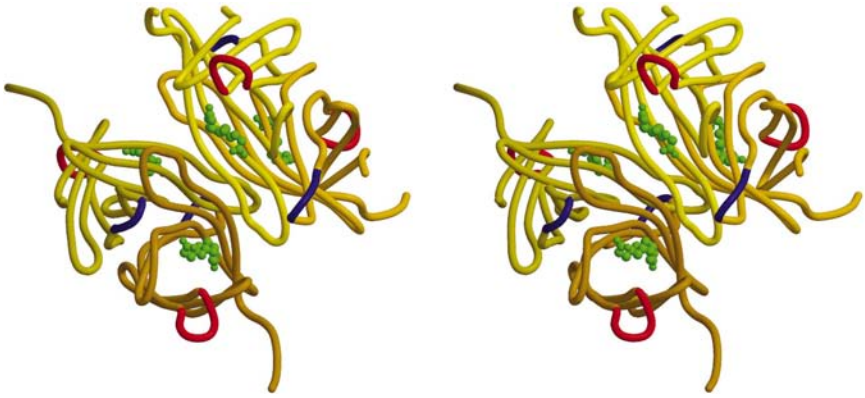

**Figure 4**
Stereoview of the streptavidin tetramer. The RGD loops are shown in blue, while flexible binding loops are shown in red. Biotin molecules bound in the ligand-binding site are shown as green ball-and-stick figures. The figure was drawn using *MOLSCRIPT* (Kraulis, 1991) and *Raster3D* (Merritt & Bacon, 1997).

**Table 3**
Intermolecular hydrogen bonds involving the RGD loops.

| | | | | Distance | |
|---|---|---|---|---|---|
| Atom | Residue | Atom | Residue | FN-SA | OPN-SA |
| NE | Arg65 | OH | Tyr83 | 2.78 | 3.04 |
| NH1 | Arg65 | O | Gly113 | 2.79 | 2.89 |
| N | Gly66 | OT1 | Ser139 | 2.69 | 2.53 |
| OD1 | Asp67 | OH | Tyr83 | 2.42 | 2.44 |

As seen in Fig. 5, the FN-SA and OPN-SA structures are very similar, except at residues 67A and 67B. Electron density for these two residues is not seen in difference electron-density maps for OPN-SA and the residues are therefore omitted from the OPN-SA model. The only amino-acid sequence difference between FN-SA and OPN-SA occurs at position 67B (see Fig. 1). The two structures are isomorphous, so it seems likely that the limited conformations available to proline restrict the polypeptide more in FN-SA and cause it to be more ordered in the crystal structure.

The refined model for FN-SA includes restrained anisotropic atomic displacement parameters (ADPs). Fig. 6 shows the thermal ellipsoids for FN-SA. The RGD loop is on the upper left and the large red ellipsoids indicate the electron density in this region is weaker and more spread out. (The other large ellipsoids are found in loops and surface residues also free to move in this crystal form.) The anisotropic ADPs in the RGD loop, when converted to isotropic temperature parameters (or *B* values), are in the range 30–40 Å$^2$. At regions ten residues on either side of the loops, the *B* values drop to 10–15 Å$^2$. Other loops in the structure have higher overall *B* values, so the RGD loops do not seem exceptional. They are simply looser and possibly more dynamic regions of these mutants. It is interesting to note that the C-terminus of the protein shows smaller ADPs near the terminus where contact is made with a neighboring molecule in the crystal. The residues just before the terminus are not as involved in intermolecular or intramolecular interactions and display more dynamic or static disorder.

A concern when discussing the dynamics or disorder of regions in a protein structure is what effect crystal-packing interactions might have on the region of interest. This is hard to assess, but it is true that for FN-SA and OPN-SA residues in the RGD loops interact with residues from neighboring molecules in the crystal. Table 3 lists the intermolecular hydrogen bonds made by these residues. No intermolecular contacts

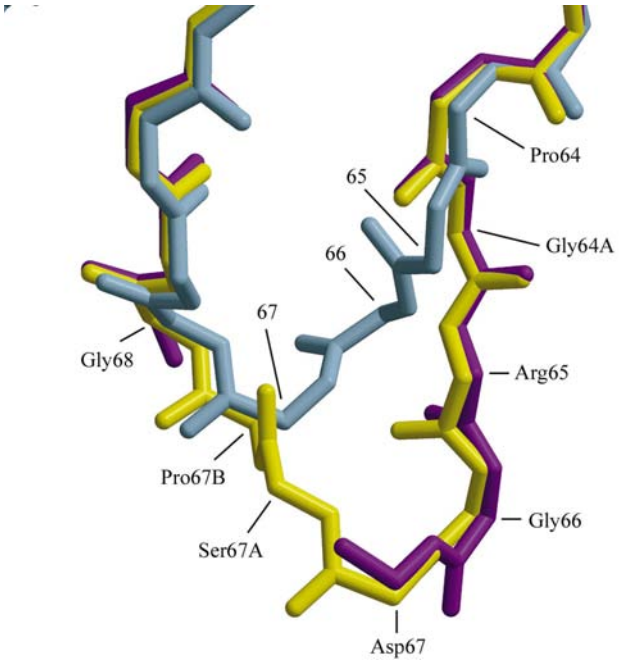


**Figure 5**
The loops of FN-SA and OPN-SA and wild-type streptavidin showing the site of addition of the RGD peptide. The superposition is as for Fig. 3. FN-SA is shown in yellow, OPN-SA is in purple and the wild type is in blue. Residues names and numbers label the $C^{\alpha}$ positions in FN-SA. The residue numbers without residue names are for wild-type streptavidin. The figure was drawn using *MOLSCRIPT* (Kraulis, 1991) and *Raster3D* (Merritt & Bacon, 1997).

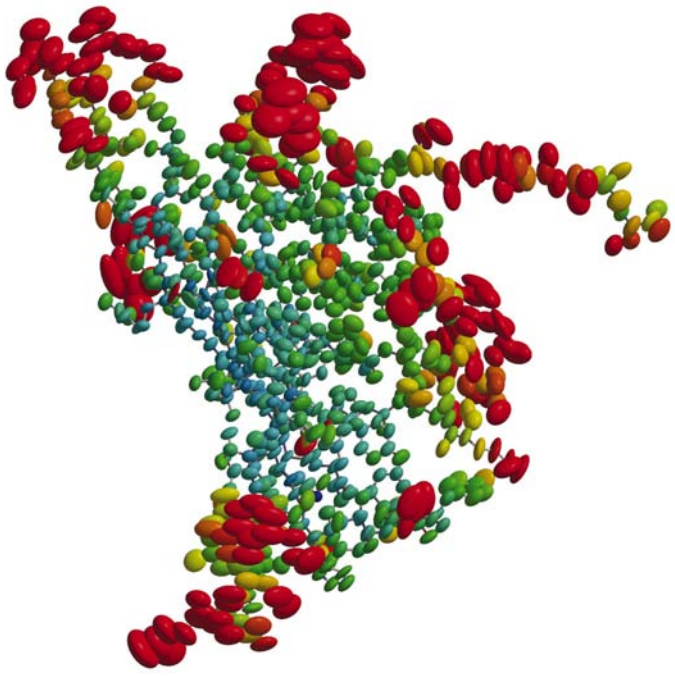

**Figure 6**
Anisotropic atomic displacement parameters (50% ellipsoids) for all atoms in FN-SA. The RGD loops are located at the upper left of the figure. ADPs with equivalent $B$ values less than 5 Å$^2$ are colored blue. Those larger than 30 Å$^2$ are colored red. The figure was drawn using *Raster3D* (Merritt & Bacon, 1997).

are made by the flanking residues 64A, 67A or 67B. The interactions involving the RGD residues will undoubtedly affect the dynamics and conformation of the RGD loop, but whether they do so in any physiologically important way is unknown. Crystal structures of different crystal forms or of complexes with integrins, the receptors for RGD sequences, as

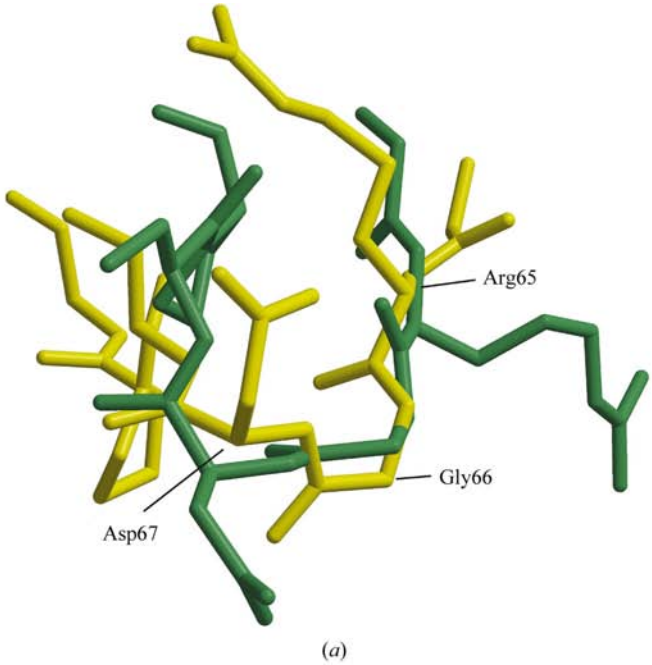


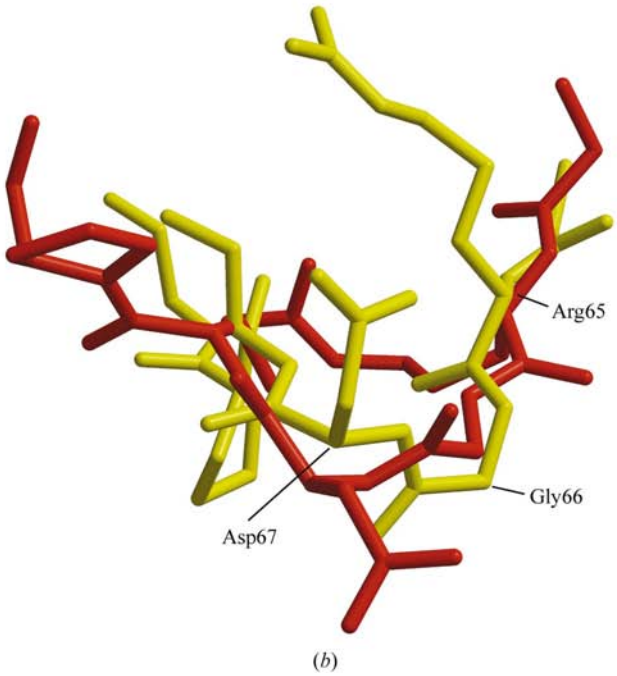


**Figure 7**
(*a*) Superposition of the RGD loop from a fibronectin module (PDB code 1fnf) onto FN-SA based on backbone atoms of the RGD residues. FN-SA in yellow, fibronectin in green. (*b*) Superposition of the RGD loop from a lysozyme mutant (PDB code 1lz6) onto FN-SA based on backbone atoms of the RGD residues. FN-SA is in yellow and lysozyme in orange. The residue names and numbers are for FN-SA. The figure was drawn using *XTALVIEW* (McRee, 1999) and *Raster3D* (Merritt & Bacon, 1997).

well as other experimental approaches will be necessary to fully determine the effects of these crystal-packing interactions.

A screening of the Protein Data Bank (November, 2001) yielded over 800 structures containing the RGD tripeptide sequence. A number of them are known to interact with integrins and are listed in Table 4. The main-chain torsion angles for the RGD residues in these models of cell-adhesion molecules are not clustered into any particular region of a Ramachandran plot (data not shown). (The torsion angles for the X-ray crystallographic entries in Table 4 are listed in Table 5.) Two selected superpositions of RGD loops from the structural models listed in Table 4 are shown in Fig. 7. Fig. 7(*a*) shows the RGD loop of fibronectin (PDB code 1fnf) superposed on the three RGD residues of FN-SA using only the $C^{\alpha}$ atoms for structural alignment. The fibronectin loop takes on a classical $\beta$-turn conformation, while the loop from FN-SA is more open without an intra-chain hydrogen bond stabilizing the loop structure. In this alignment, the side chains of the arginine and aspartic acid residues do not overlap well. It is not clear how the two conformations seen here for the RGD sequence can bind to the same receptor site. A superposition of a lysozyme mutant containing an engineered RGD tripeptide (PDB code 1lz6) onto FN-SA is presented in Fig. 7(*b*). The loop in lysozyme is further opened and bulges from the side of the protein. The side-chain torsion angles for this engineered RGD loop again differ from those found in FN-SA.

**Table 4**
PDB entries with cell-adhesion properties.

| PDB code | Protein | Method | Reference |
|---|---|---|---|
| 1dki | Streptcoccal pyrogenic exotoxin B | X-ray | Kagawa *et al.* (2000) |
| 1fna | Fibronectin type-III domain | X-ray | Dickinson *et al.* (1994) |
| 1fnf | Fibronectin domains | X-ray | Leahy *et al.* (1996) |
| 1fuv | RGD peptide isomer A | NMR | Assa-Munt *et al.* (2001) |
| 1ful | RGD peptide isomer B | NMR | Assa-Munt *et al.* (2001) |
| 1lz5 | Lysozyme containing an RGD sequence | X-ray | Yamada *et al.* (1993) |
| 1lz6 | Lysozyme containing an RGD sequence | X-ray | Yamada *et al.* (1993) |
| 1mfn | Fibronectin | NMR | Copie *et al.* (1998) |
| 1ten | Tenascin (fibronectin type-III repeat) | X-ray | Leahy *et al.* (1992) |
| 1ttf | Fibronectin type-III module | NMR | Baron *et al.* (1992) |
| 1ttg | Fibronectin type-III module | NMR | Main *et al.* (1992) |
| 2ech | Echistatin | NMR | Atkinson *et al.* (1994) |
| 2mfn | Fibronectin | NMR | Berman *et al.* (2000) |

**Table 5**
Main-chain torsion angles for RGD residues in selected cell-adhesion molecules from the PDB.

| | Arginine | | | Glycine | | | Aspartic acid | | |
|---|---|---|---|---|---|---|---|---|---|
| PDB code | $\varphi$ | $\psi$ | $\omega$ | $\varphi$ | $\psi$ | $\omega$ | $\varphi$ | $\psi$ | $\omega$ |
| 1mm9 (FN-SA) | −148.6 | 137.6 | −172.1 | −77.8 | −26.8 | −175.6 | −86.9 | −11.5 | −173.3 |
| 1moy (OP-SA) | −139.9 | −162.1 | 179.0 | −109.5 | 6.8 | 177.1 | −128.4 | n/a | n/a |
| 1fnf | −142.1 | −170.2 | −179.0 | 80.6 | −163.8 | −179.2 | −75.4 | −24.2 | 178.8 |
| 1fna | −115.6 | 5.6 | 177.1 | 142.8 | 121.6 | −178.0 | −100.7 | 127.1 | −179.7 |
| 1ten | −158.3 | 99.6 | 179.6 | 63.4 | −118.7 | −179.5 | −75.4 | −25.2 | −178.4 |
| 1lz5 | −139.9 | 117.6 | 179.8 | 178.6 | −162.7 | 178.9 | −98.9 | 121.1 | −178.9 |
| 1lz6 | 174.2 | 146.5 | 178.2 | 134.6 | 94.1 | −179.7 | 83.6 | 35.8 | −177.0 |
| 1dki† | −55.8 | −39.6 | −178.6 | −66.5 | −11.0 | −179.8 | −96.9 | −0.3 | −178.5 |
| | 4.8 | −76.4 | −149.7 | 14.2 | −70.6 | −141.9 | 8.0 | −84.2 | −126.9 |
| | 5.7 | −75.1 | −148.6 | 14.6 | −71.1 | −138.3 | 12.3 | −84.7 | −130.3 |
| | 5.1 | −77.1 | −145.2 | 17.0 | −68.6 | −136.4 | 11.8 | −89.0 | −135.2 |

† There are four molecules in the asymmetric unit for PDB entry 1dki.

These comparisons are representative in that no obvious similarities are found in the conformations of the RGD loops in the structures listed in Table 4. A range of structures are observed for the loops; if they are physiologically important, there must be considerable variation in the complementary receptor sites for the RGD motif. Another view would be that the observed conformations represent frozen or trapped structures of dynamic loops that sample a large portion of conformational space and occasionally take on conformations suitable for binding to the receptors. Experimental information about the conformation of the loops in complex with their receptors will be needed to choose between these alternatives.

## 4. Conclusions

Two streptavidin mutants have been generated with cell-adhesion properties (McDevitt *et al.*, 1999) by modifying one of the surface loops of wild-type streptavidin to contain an RGD (argininine-glycine-aspartic acid) sequence. Residues flanking the RGD peptide were also altered to generate one mutant with a fibronectin-like RGD loop and one with an osteopontin-like loop. The two molecules differ in sequence two amino acids beyond the RGD peptide. One contains a proline (FN-SA) and one contains a valine (OPN-SA). The crystals of the two mutants are isomorphous, but the electron density for the latter structure is too weak for the valine and an adjacent residue for them to be added to the structural model. This disorder may be associated with the dynamics of RGD loops and their ability to bind to receptors and control cell adhesion. Comparison with other published cell-adhesion molecule structures containing RGD sequences indicates that these loops can take on a broad range of conformations, either indicating that a correspondingly large set of receptor-binding sites exists or that structural flexibility allows the molecules to sample the limited conformations recognized by the receptors.

This work was supported by NIH grant DK-49655. Portions of this research were carried out at the Stanford Synchrotron Radiation Laboratory, a national user facility operated by Stanford University on behalf of the US Department of Energy, Office of Basic Energy Sciences. The SSRL Structural Molecular Biology Program is supported by the Department of Energy, Office of Biological and Environmental Research

and by the National Institutes of Health, National Center for Research Resources, Biomedical Technology Program and the National Institute of General Medical Sciences.

## References


Assa-Munt, N., Jia, X., Laakkonen, P. & Ruoslahti, E. (2001). *Biochemistry*, **40**, 2373–2378.

Atkinson, R. A., Saudek, V. & Pelton, J. T. (1994). *Int. J. Pept. Protein Res.* **43**, 563–572.

Barbas, D. F. III, Languino, L. R. & Smith, J. W. (1993). *Proc. Natl Acad. Sci. USA*, **90**, 10003–10007.

Baron, M., Main, A. L., Driscoll, P. C., Mardon, H. J., Boyd, J. & Campbell, I. D. (1992). *Biochemistry*, **31**, 2068–2073.

Berman, H. M., Westbrook, J., Feng, Z., Gilliland, G., Bhat, T. N., Weissig, H., Shindyalov, I. N. & Bourne, P. E. (2000). *Nucleic Acids Res.* **28**, 235–242.

Brünger, A. T. (1992). *Nature (London)*, **355**, 472–475.

Copie, V., Tomita, Y., Akiyama, S. K., Aota, S., Yamada, K. M., Venable, R. M., Pastor, R. W., Krueger, S. & Torchia, D. A. (1998). *J. Mol. Biol.* **277**, 663–682.

Dickinson, C. D., Veerapandian, B., Dai, X.-P., Hamlin, R. C., Xuong, N.-H., Ruoslahti, E. & Ely, K. R. (1994). *J. Mol. Biol.* **236**, 1079–1092.

Engh, R. A. & Huber, R. (1991). *Acta Cryst.* A**47**, 392–400.

Freitag, S., Le Trong, I., Klumb, L., Stayton, P. S. & Stenkamp, R. E. (1997). *Protein Sci.* **6**, 1157–1166.

Hashino, K., Shimojo, T., Kimizuka, F., Katao, I., Maeda, T., Sekiguchi, K. & Titani, K. (1992). *J. Biochem.* **112**, 547–551.

Hendrickson, W. A., Pahler, A., Smith, J. L., Satow, Y., Merritt, E. A. & Phizackerley, R. P. (1989). *Proc. Natl Acad. Sci. USA*, **86**, 2190–2194.

Kagawa, T. F., Cooney, J. C., Baker, H. M., McSweeney, S., Liu, M. Y., Gubba, S., Musser, J. M. & Baker, E. N. (2000). *Proc. Natl Acad. Sci. USA*, **97**, 2235–2240.

Kraulis, P. J. (1991). *J. Appl. Cryst.* **24**, 946–950.

Leahy, D. J. (1997). *Ann. Rev. Cell Devel. Biol.* **13**, 363–393.

Leahy, D. J., Aukhil, I. & Erickson, H. P. (1996). *Cell*, **84**, 155–164.

Leahy, D. J., Hendrickson, W. A., Aukhil, I. & Erickson, H. P. (1992). *Science*, **258**, 997–991.

McDevitt, T. C., Nelson, K. E. & Stayton, P. S. (1999). *Biotechnol. Prog.* **15**, 391–396.

McRee, D. E. (1999). *J. Struct. Biol.* **125**, 156–165.

Maeda, T., Oyama, R., Ichihara-Tanaka, K., Kimizuka, F., Kato, I., Titani, K. & Sekiguchi, K. A. (1989). *J. Biol. Chem.* **264**, 15165–15168.

Main, A. L., Harvey, T. S., Baron, M., Boyd, J. & Campbell, I. D. (1992). *Cell*, **71**, 671–678.

Matthews, B. W. (1968). *J. Mol. Biol.* **33**, 491–497.

Merritt, E. A. & Bacon, D. J. (1997). *Methods Enzymol.* **277**, 505–524.

Otwinowski, Z. & Minor, W. (1997). *Methods Enzymol.* **276**, 307–326.

Pytela, R., Pierschbacher, M. D. & Ruoslahti, E. (1985). *Proc. Natl Acad. Sci. USA*, **82**, 5766–5770.

Rossi, F., Billeta, R., Ruggeri, A. & Zanetti, M. (1995). *Mol. Immunol.* **32**, 341–346.

Ruoslahti, E. (1991). *J. Clin. Invest.* **87**, 1–5.

Ruoslahti, E. & Pierschbacher, M. D. (1987). *Science*, **238**, 491–497.

Sheldrick, G. M. & Schneider, T. R. (1997). *Methods Enzymol.* **277**, 319–343.

Smith, J. W., Tachias, K. & Madison, E. L. (1995). *J. Biol. Chem.* **270**, 30486–30490.

Weber, P. C., Ohlendorf, D. H., Wendoloski, J. J. & Salemme, F. R. (1989). *Science*, **243**, 85–88.

Yamada, T., Matsushima, M., Inaka, K., Ohkubo, T., Uyeda, A., Maeda, T., Titani, K., Sekiguchi, K. & Kikuchi, M. (1993). *J. Biol. Chem.* **268**, 10588–10592.